Study of the size-dependent properties of Sc_nAl (n = 1–14) clusters by density-functional theory

2009 J. Phys.: Condens. Matter 21 046004

(http://iopscience.iop.org/0953-8984/21/4/046004)

J. Phys.: Condens. Matter **21** (2009) 046004 (7pp) doi:10.1088/0953-8984/21/4/046004

Study of the size-dependent properties of Sc_nAl ($n = 1$–14) clusters by density-functional theory

Mei Wang, Guoli Qiu, Xiaowei Huang, Zuliang Du and Yuncai Li

Key Laboratory for Special Functional Materials, Ministry of Education, Henan University, Kaifeng 475001, People's Republic of China

E-mail: liyuncai@henu.edu.cn

Received 26 September 2008, in final form 14 November 2008
Published 8 January 2009
Online at stacks.iop.org/JPhysCM/21/046004

Abstract

The geometries, stabilities, and electronic and magnetic properties of Sc_nAl ($n = 1$–14) clusters with different spin configurations have been investigated systematically within the framework of the gradient-corrected density-functional theory. Our resulting geometries show that the aluminum atom remains on the surface of clusters with $n < 9$, while it takes up the center of Sc-cage clusters with $n \geqslant 9$. Besides, the doping of Al improves the stability of the host clusters. Maximum peaks are observed for Sc_nAl clusters at $n = 3$, 6, 10 and 12 with the size dependent on the second-order energy differences and fragmentation energies, implying that these clusters are relatively more stable. For all the Sc_nAl clusters studied, we find the charge transfer from Sc to Al sites and the coexistence of ionic and covalent bonding characteristics. The doping of the Al atom induces the magnetic moments of the host clusters decrease except for $n = 8$ and 14 and the total magnetic moments are quenched at $n = 5$, 7, 9 and 11.

1. Introduction

Due to the existence of d electrons, the structure and magnetic properties of transition metal (TM) clusters have received considerable attention, and a variety of interesting magnetic behaviors different from those of the corresponding bulk solids have been identified [1–6]. For example, a transition from ferromagnetic to ferrimagnetic Mn–Mn coupling is observed at $n = 5$ for Mn_n clusters and the ferrimagnetic states continue to be the ground state for larger clusters, even though Mn is antiferromagnetic in the bulk phase [7, 8]. Recently, TM nanoalloy clusters have received considerable attention for their peculiar catalytic, optical, magnetic, electronic and geometric properties [9–15]. Axel Pramann *et al* have confirmed the high stability of the $Co_{12}V$ cluster with a most plausible icosahedral structure and the V atom in the cage center by anion photodetachment photoelectron spectroscopy [16]. For the Ni_nB clusters, the different gap between the two (spin-up and spin-down) electron states indicates it can be used in the spin-polarized transport systems [17]. Theoretically, some attempts have been done on Ti_nAl clusters [18], Ni_nAl clusters [19, 20], Mn_xCo_y clusters [21] and so on. For such clusters, chemical and physical properties can be tailored by varying not only the size but also the composition for a specific purpose. This opens the way to a large variety of potential applications in some areas such as high-density recording, catalysis, optics, etc. In particular, the interest in TM clusters arises from a desire to seek a solution to the technologically important question: how do magnetic properties change in reduced dimensions? The candidates chosen for the present study, Sc and Al, have very interesting properties in low dimensions.

As with most transition elements, scandium is paramagnetic in its bulk phase, but the relatively high paramagnetic susceptibilities, as compared to those of its neighbors, suggest that it is on the verge of ferromagnetic instability, and may be induced to display magnetic ordering by spatial confinement. Moreover, recent Stern–Gerlach molecular-beam deflection studies have shown that small scandium clusters are magnetic ordering in the range of $n = 5$–20 and the magnetic moment is as high as $6.0 \pm 0.2\ \mu_B$ for the Sc_{13} cluster [22]. Yuan *et al* [23] and Wang [24] have studied the evolution of structural, electronic and magnetic properties of small Sc_n clusters using first-principles density-functional theory (DFT). Recently, Tian *et al* [25] have investigated the geometry and electronic structures of Sc_nAl clusters but the size was limited

Table 1. Calculated bond length (Å), binding energy E_b (kcal mol^{-1}), spin multiplicity and vibrational frequencies ω (cm^{-1}) of the Sc_2 dimer in the ground state.

Functional	Bond length	E_b	Multi	ω
PW91	2.602	36.674	5	245.23
PBE	2.610	38.366	5	261.78
BLYP	2.580	40.674	5	253.24
LSDA	2.549	45.230	1	229.48
Expt		25.9 ± 5[a]	5[b]	239.9[c]

[a] Reference [26]. [b] Reference [27]. [c] Reference [28].

($n = 1$–8, 12). In this paper, we study the size-dependent structural, electronic and magnetic properties of Sc_nAl ($n = 1$–14) clusters by the DFT-based first-principles method, and the pure scandium clusters are also studied for comparison. This paper is organized as follows: in section 2, we describe briefly the computational methods employed in this work. In section 3, the theoretical lowest-energy structures of Sc_nAl clusters are given and the growth behavior, relative stabilities, highest occupied molecular orbital (HOMO)–lowest unoccupied molecular orbital (LUMO) gaps and magnetic properties of the Sc_nAl ($n = 1$–14) clusters are computed and discussed in detail. The conclusion is given in section 4.

2. Theoretical methods

The reliability of DFT studies depends on the choice of the functional and the basis set. To some extent, the basis set and the exchange–correlation function can affect the calculation results, especially for magnetic properties. As a test of the computational method, we perform the calculations on Sc_2 dimers using several exchange–correlation functionals. For each functional, a basis set composed of double numerical basis with d-polarization functions (DND) is used, and all-electron spin-unrestricted calculations are performed. The bond length, binding energy, spin multiplicity and frequency, and the corresponding experimental results for Sc_2 dimers, are summarized in table 1. It is obvious that the results obtained by the PW91 exchange–correlation functional [29] are closest to the experimental data.

In addition, the bond length (2.641 Å), average binding energy (0.982 eV) and vibrational frequency (319.7 cm^{-1}) of the Al_2 dimer are calculated using the PW91 functional and DND basis set, and the results are in good agreement with the experimental values of 2.560 Å, 0.997 ± 0.108 eV and 350.01 cm^{-1} [30], respectively. This indicates that our approach is efficient and reliable in studying small Sc_nAl clusters. Thus, the density functional is treated with the generalized gradient approximation using the PW91 functional. An octuple scheme is used for the multipolar fitting procedure, while a fine grid scheme is used for numerical integration, aiming at accurately evaluating the charge density. The convergence criterion of optimization is set as 1×10^{-5} eV Å^{-1} for the energy gradient and 5×10^{-4} Å for the atomic displacement. All calculations are carried out with the Dmol^3 package [31]. It is noteworthy that we perform natural orbital population analysis (NPA) on the ground state structures. Because NPA computation is not available in the DMOL package, we use the PW91 functional and the LANL2DZ basis set [32] implemented in the GAUSSIAN-03 package [33].

In order to obtain the lowest-energy structures of Sc_nAl clusters, we consider possible isomeric structures by placing the Al atom on each possible site of the Sc_n cluster as well as by substituting one Sc atom by the Al atom from the Sc_{n+1} cluster. Simultaneously, the most energetically favorable geometries of Al-doped other TM clusters published in the literature, for example Ti_nAl [18] and Y_nAl [34], are taken as a guide. For a given initial structure, the harmonic vibration frequencies are also calculated so as to verify the nature of the stationary point on potential energy surfaces. In this paper, spin-unrestricted calculations are performed for all allowable spin multiplicities. We start with a spin singlet configuration for the even-electron systems and a spin doublet configuration for the odd-electron systems until the energy minimum is reached.

3. Results and discussion

3.1. Equilibrium geometries of Sc_nAl ($n = 1$–14) clusters

Using the computation scheme described in section 2, the lowest-energy structures and some metastable low-energy isomers of Sc_{n+1} and Sc_nAl ($n = 1$–14) clusters are presented in figure 1; meanwhile the symmetry, spin multiplicity, binding energy, HOMO–LUMO gap, the magnetic moment and the charge of the Al atom of Sc_nAl clusters for the lowest-energy structures are listed in table 2. It is found that the Al atom occupies a peripheral position for $n < 9$, which could be well understood by taking into account the atomic radii of the constituent atoms and relative strength of bonds. Namely, the monovalent Al atom has a larger Pauling ionic radius than the Sc atom, and the Sc–Al bond is weaker than the Sc–Sc bond in the corresponding diatomic system. Therefore, the Al atom prefers remaining on the surface to favor the stability of the system, whereas, beyond $n = 9$, the Al atom is trapped within the cage of Sc host atoms, leading to an evolution towards an icosahedral structure. Such a change in the position of the impurity atom has also been observed in Ti_nAl [18] and Y_nAl [34] clusters. And it might be reasonable that trivalent Al has a much smaller Pauling ionic radius than Sc atoms, and this is beneficial to facilitating the monovalent to trivalent transition of the valence of the Al atom in Sc_nAl clusters.

As shown in figure 1, for the ScAl monomer with a $C_{\infty v}$ symmetry, the binding energy and vibration frequency are calculated to be 2.054 eV and 251.43 cm^{-1}, respectively. The optimized results indicate that the singlet spin state is the most stable structure, and lower by 0.011 eV in energy than the triplet state. For Sc_2Al, the lowest-energy structures, isosceles triangles (C_{2v}) with an Al atom at the apex, can be thought of as that of the corresponding pure Sc_n clusters after being mono-substituted by a single Al atom, and the bond length of the isosceles (2.650 Å) is shorter than that of the hemline (2.900 Å). The energy of the doublet state is lower than that of the quartet state only by 0.138 eV. As expected, the two linear chains of Sc_2Al (not shown) are metastable isomers, and the

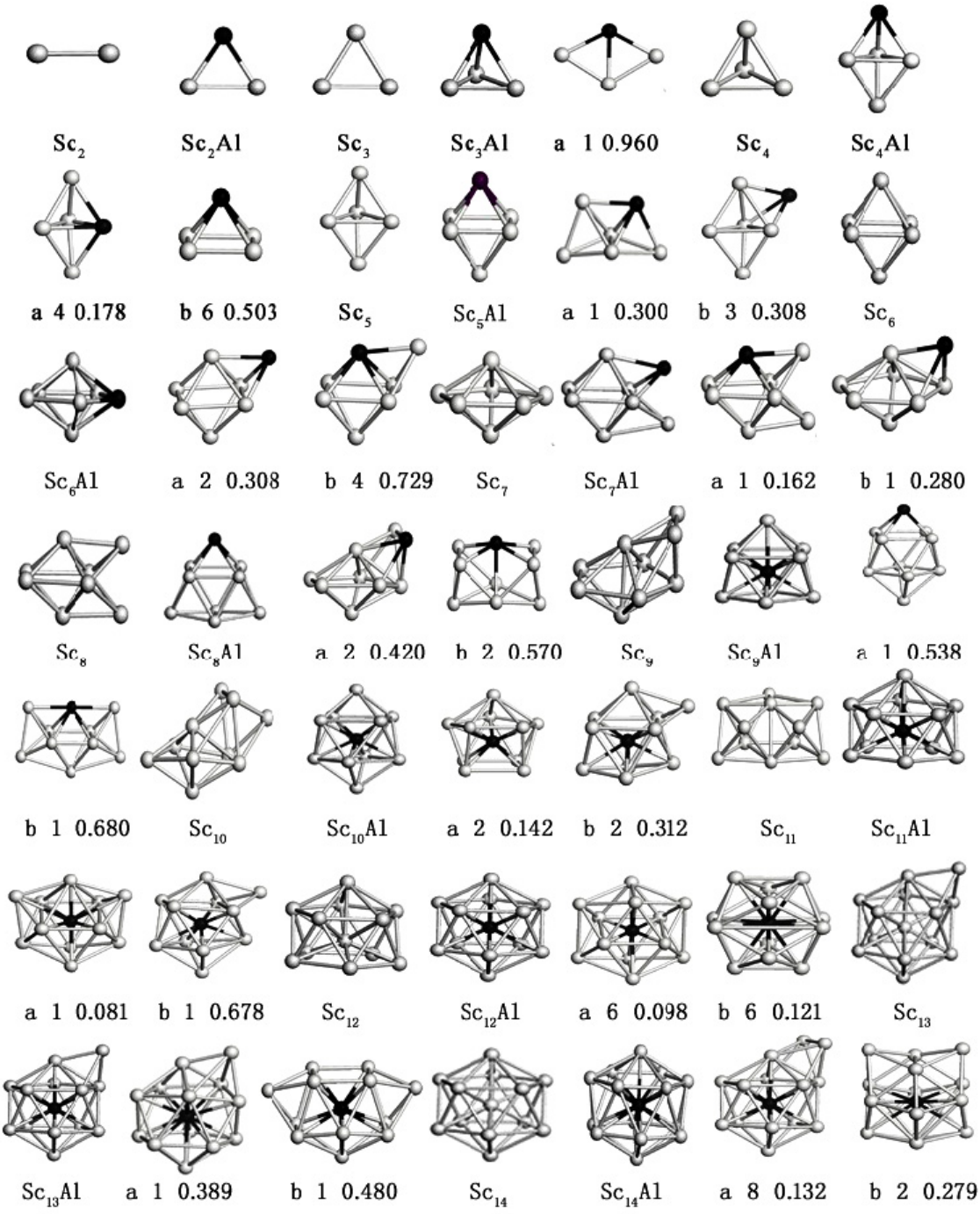

Figure 1. Equilibrium geometries of Sc_{n+1} and Sc_nAl clusters, and the low-lying energy isomers ((a), (b)) for doped clusters. The numbers represent the multiplicity and difference in total energy (eV) from the corresponding ground state, respectively. The gray and black balls represent Sc and Al atoms, respectively.

binding energy of the chain with the Al atom at the terminal position is lower than that of the chain with a central Al atom by 0.282 eV. At $n = 3$, the first three-dimensional structure emerges and its lowest-energy structure with a spin singlet state is a tetrahedral configuration (C_{3v}), which can be generated by substituting one Sc atom at one apex of the pyramid of the Sc_4 frame with one Al atom. For the planar rhombic isomer, the total energy of the triplet state is higher than that of the ground state by 0.960 eV. The lowest-energy structure of the Sc_4Al cluster with a state is a triangular bipyramid (C_{3v}) with an Al atom on the vertex. The doublet state is found to be more stable than the quartet state and the energy of the doublet state is lower than that of the quartet state by 0.070 eV. The energy of the low-lying energy structure with C_{2v} symmetry in which the Al atom lies at the triangular ring is higher than that of the ground state structure by 0.178 eV. In the case of Sc_5Al, the lowest-energy structure is an octahedron (C_{4v}) with the Al atom at one apex, and the energy of the spin singlet is lower than

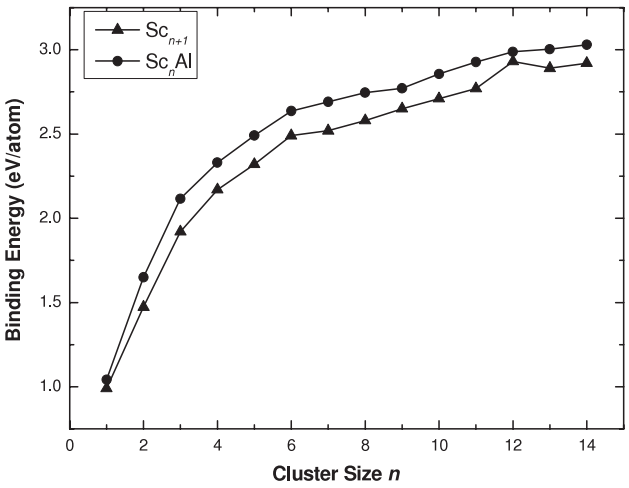

Figure 2. Size dependence of the average binding energy of Sc_{n+1} and Sc_nAl clusters.

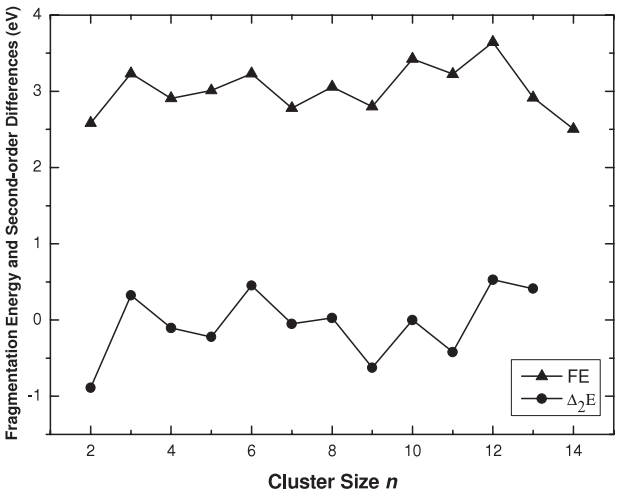

Figure 3. Size dependence of the fragmentation energy and the second-order energy differences of Sc_nAl clusters.

Table 2. The symmetry S, spin multiplicity 'Multi', total magnetic moment M (μ_B), binding energy per atom E_b (eV), HOMO–LUMO gap E_g (eV), magnetic moment M (Al) (μ_B) and charge Q (Al) of the Al atom of Sc_nAl clusters for the lowest-energy structures.

n	S	Multi	M	M (Al)	E_b	E_g	Q (Al)
1	$C_{\infty v}$	1	2	0.664	1.042	0.848	−0.069
2	C_{2v}	2	1	0.182	1.650	0.465	−0.399
3	C_{3v}	1	2	0.006	2.116	0.275	−0.438
4	C_{3v}	2	1	0.141	2.330	0.226	−0.352
5	C_{4v}	1	0	0	2.491	0.416	−0.279
6	C_{2v}	2	1	0.001	2.637	0.100	−0.294
7	C_s	1	0	0	2.690	0.035	−0.317
8	C_{2v}	4	3	−0.022	2.745	0.115	−0.327
9	C_{4v}	1	0	0	2.771	0.203	−0.851
10	D_{4d}	2	1	−0.013	2.856	0.051	−0.751
11	C_{5v}	1	0	0	2.927	0.098	−0.348
12	I_h	6	5	−0.231	2.988	0.226	−0.387
13	C_{3v}	1	2	−0.084	3.003	0.028	−0.396
14	D_{6d}	8	7	−0.199	3.052	0.086	−0.325

that of the triplet state by 0.039 eV. For Sc_6Al, a pentagonal bipyramid (C_{2v}) with an Al atom as a part of the pentagonal ring in a doublet state is more stable than a similar structure in a quartet state; the energy benefit is 0.047 eV. In addition, capped octahedron, tricapped tetrahedron and bicapped square pyramid are considered. However, these isomers have higher energy than the ground state structure. The energies of the second and third lowest-energy isomers (in figure 1) are 0.308 and 0.729 eV higher than that of the ground state, respectively. For the Sc_7Al cluster, the bicapped tetragonal bipyramid (C_s) with a singlet state, similar to that of Sc_8, has the lowest total energy. Its energy is energetically lower than that of the same structure with the spin triplet by 0.032 eV. The most stable structure of Sc_8Al is the mono-capped tetragonal antiprism structure (C_{2v}) with a quartet state. The spin quartet is nearly degenerate with the doublet state, with the energy difference of 0.029 eV.

The structural transition takes place at $n = 9$. The first trapped structure appears at $n = 9$ and it evolves towards an icosahedron beyond $n = 9$. For Sc_9Al, the Al atom can be supposed to be located at the center of the Sc_9 frame, and the spin singlet state is found to be the most stable. The ground state geometry of the $Sc_{10}Al$ cluster with a doublet state can be thought of as a substituted structure of Sc_{11}, which is similar to the ground state geometries of $Ti_{10}Al$ [18] and $Y_{10}Al$ [34] clusters. The multi-rhombic concave $Sc_{10}Al$ with C_{2v} symmetry is nearly degenerate with the lowest-energy configuration (0.142 eV). The most stable structure of $Sc_{12}Al$ is an icosahedral structure, and the Al atom is located in the center of the Sc cage in this case. Besides, the structures of $Sc_{11}Al$ and $Sc_{13}Al$ can be obtained by removing one Sc atom from the icosahedron of $Sc_{12}Al$ or by capping one Sc atom to the same icosahedron. Interestingly, the isomer structure clusters are also icosahedral-like structures, indicating that the icosahedral structures dominate the potential surface of the Sc_nAl clusters around $n = 12$. The energy of $Sc_{12}Al$ with a sextet state is lower than that of the quartet and octet states by 0.038 and 0.054 eV, respectively. Two energetically degenerate isomers (a and b) having the same spin multiplicities are obtained. They lie at only 0.098 and 0.121 eV higher in energy, respectively. The most stable structure of $Sc_{14}Al$ with a octet state is a bicapped hexagonal antiprism with D_{6d} symmetry. The quartet and sextet states are higher in energy by 0.055 and 0.036 eV, respectively. The next two stable isomers are found to be a bicapping on adjacent faces on an icosahedron (a) and a bicapping on an hcp structure (b). Their energies are only 0.132 and 0.279 eV above the ground state, respectively.

3.2. Binding energy

In order to understand the relative stability of the Sc_nAl clusters, we present the average binding energy per atom, the fragmentation energy and the second-order differences of energies in figures 2 and 3, respectively. As shown in figure 2, the average binding energies of the Sc_nAl clusters increase monotonically with the cluster size. Compared to the Sc_{n+1} clusters, the doping of the Al atom enhances the binding energy of the host clusters, which implies the doping of the Al atom improves the stability of Sc_n clusters. This is consistent with

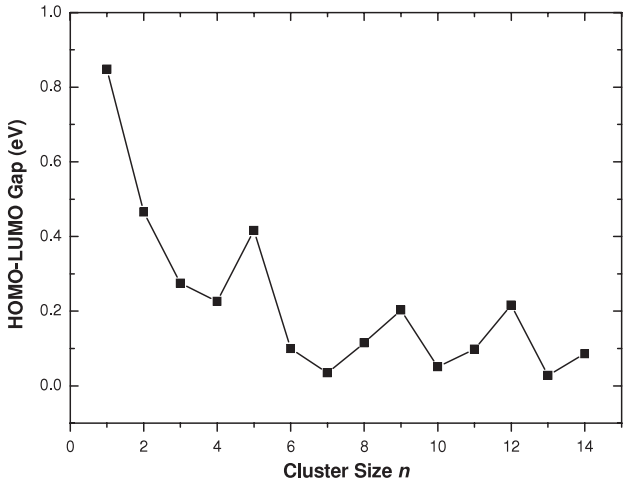

Figure 4. Size dependence of the HOMO–LUMO gaps of Sc_nAl clusters.

the result reported in [25]. From figure 2, it is difficult to predict the Sc_nAl clusters which are more stable than others, as has been demonstrated clearly for simple metal clusters such as the alkali series. Thus, to study if any of these Sc_nAl clusters could be magic, we will investigate the second differences of total energies.

Figure 3 shows the fragmentation energy and the second-order differences of total energies. The fragmentation energy $[D(n, n-1)]$ and the second-order differences of energies $[\Delta_2 E]$ are defined as

$$D(n, n-1) = E(Sc_{n-1}Al) + E(Sc) - E(Sc_nAl),$$

$$\Delta_2 E(n) = E(Sc_{n+1}Al) + E(Sc_{n-1}Al) - 2E(Sc_nAl)$$

where $E(\cdots)$ is the total energy of the corresponding system. As shown in figure 3, the local abundant peaks of $D(n, n-1)$ appear at $n = 3$, 6, 10 and 12, and the maxima of second-order differences of energies are also observed for the same systems, indicating that they are more stable than their neighbors. Therefore, it can be concluded that $n = 3$, 6, 10 and 12 are the magic numbers of Sc_nAl ($n = 1$–14) clusters. The behavior of the variations is different to those of alkali and noble clusters which exhibit characteristic shell oscillations with respect to the cluster size. Obviously, the stable clusters originate mainly from the compact atomic arrangements, and this definition can be easily illustrated by the $Sc_{12}Al$ cluster. For the $Sc_{12}Al$ cluster, the icosahedron is well established and has been observed frequently as a geometric magic number. Furthermore, it holds 39 cluster valence electrons and still loses one electron to form the electronic magic numbers (8, 20, 40, etc). Therefore, it suggests an important role of the geometrical compact arrangements of their stabilities.

3.3. HOMO–LUMO gap

The HOMO–LUMO gap, as a characteristic quantity of a metal cluster-matrix electronic structure, reflects the ability for clusters to undergo activated chemical reactions with small molecules. Generally speaking, the magic clusters mostly have a very large HOMO–LUMO gap for the metal clusters. However, we do not find a strong correlation between the HOMO–LUMO gap and the energetic stability of the Sc_nAl clusters. As shown in figure 4, the HOMO–LUMO gap reaches a maximum at $n = 5$, 9 and 12, implying that these three clusters have stronger chemical stability than their neighbors. From table 2, it is seen that the HOMO–LUMO gaps are relatively small (around 0.1–0.3 eV) for all of the Sc_nAl clusters containing more than six atoms. This might be cited as one of the indicators of metallic behavior, appearing even in very small clusters.

To investigate the nature of bonding in these clusters, we have performed detailed analysis of the molecular orbitals by examining the partial density of states from the contribution of different orbital components (s, p, d) and the electron density of the HOMO and LUMO states. Detailed analyses of the electronic levels show that the HOMO and LUMO are mainly composed of Sc s and d states mixed with the Al p state, and the contribution from the Al s state is very little. In figure 5, we present the distribution of electron density of HOMO and LUMO states of some Sc_nAl clusters. One can see that both the HOMO and LUMO states are mainly localized around Sc atoms, and there is also some distribution around the Al atom. The electronic states in the vicinity of the Fermi level come mainly from the s, p and d states. It means that all the HOMO and LUMO states are nondegenerate and delocalized.

3.4. Magnetic properties

Based on the optimized geometries, the average magnetic moment per atom for Sc_nAl ($n = 1$–14) clusters is also computed to investigate the size dependence, using the computed magnetic moment of Sc_{n+1} ($n = 1$–14) as a comparison, and the results are shown in figure 6. It can be seen that the average magnetic moments of Sc_{n+1} and Sc_nAl clusters oscillate with increasing size. For Sc_{n+1} clusters, maxima are found at $n = 2$, 4, 6, 8, 10 and 13, which are in general agreement with the previous work [23, 24]. But, for Sc_{13} with I_h symmetry, the magnetic moment is 15 μ_B, lower than the results (15 μ_B) of [23, 24]. This is attributed to the differences in the computational details. The doping of the Al reduces the average magnetic moments of the host Sc_n clusters except for $n = 8$ and 14. Moreover, for Sc_5Al, Sc_7Al, Sc_9Al and $Sc_{11}Al$ clusters, the average magnetic moments are completely quenched due to the spin exchange effect of the itinerant 3d electrons disappearing after doping the Al. It needs to be mentioned that the magnetic moment is equal to zero for Sc_3Al in [25], but our result is 2 μ_B. The even–odd alternation (the Sc_nAl clusters have total magnetic moments 1 μ_B for $n = 2$, 4 and 6, but 2 μ_B for $n = 1$, 3 and 13 presented in table 1) in cluster magnetism may be attributed to the odd number of valence electrons.

In order to further study the magnetic property of the Sc_nAl clusters, we put up a detailed analysis on the onsite atomic charges and local magnetic moments of Sc and Al in table 3. For Sc_n clusters, 4s electrons of Sc are mainly transferred to the 3d orbit, which enhances the spin exchange effect of the itinerant 3d electron and result in the enhancement

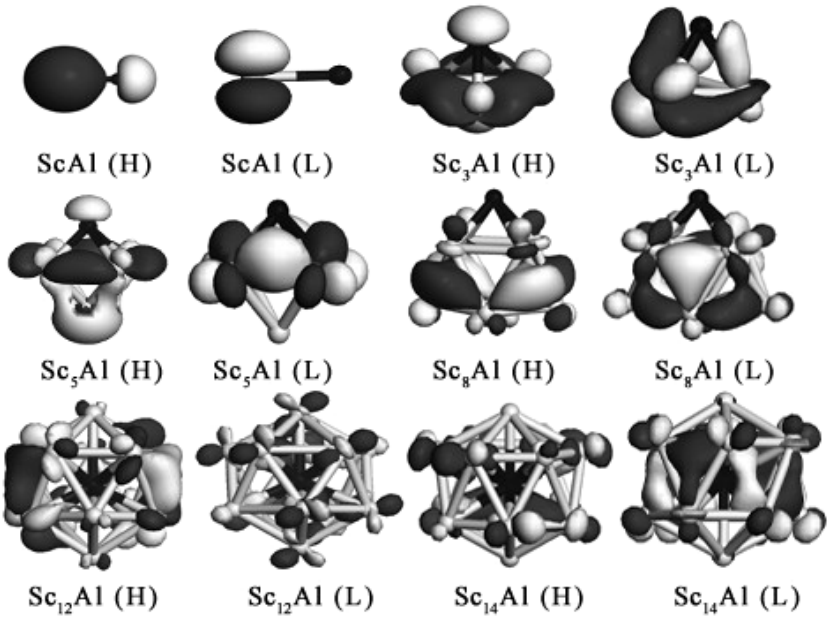

Figure 5. The HOMO and LUMO orbitals of Sc_nAl clusters.

Table 3. The charge $Q(e)$ and local magnetic moment M (μ_B) of 3s and 3p states for Al atom and 3d, 4s, 4p states for Sc in Sc_nAl and Sc_{n+1} ($n = 1, 8, 12$) clusters.

	Al				Sc					
	3s		3p		3d		4s		4p	
Cluster	Q	M	Q	M	Q	M	Q	M	Q	M
ScAl	1.95	0.012	1.12	0.629	1.47	1.358	1.42	−0.008	0.04	0.047
Sc_2					1.97	1.547	1.00	0.338	0.04	0.093
Sc_8Al	1.55	−0.005	1.77	−0.020	1.60–2.15	1.114	0.86–1.05	−0.018	0.04–0.06	0.082
Sc_9					1.68–2.86	0.478	0.82–1.02	0.031	0.02–0.05	0.066
$Sc_{12}Al$	1.46	−0.058	1.92	−0.184	1.83	0.412	1.10	−0.014	0.04	0.036
Sc_{13}					1.92–4.39	12.016	0.77–0.86	1.389	0.02–0.04	1.348

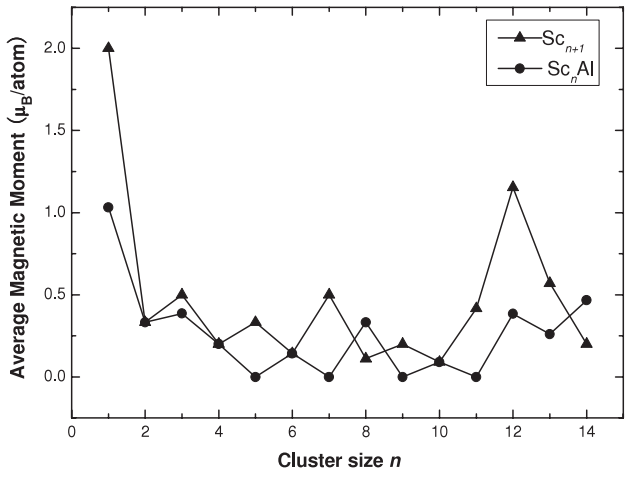

Figure 6. Size dependence of the magnetic moments of Sc_{n+1} and Sc_nAl clusters.

of the magnetic moment. For Sc_nAl clusters, 4s electrons of Sc are transferred not only to its own 3d and 4p orbitals but also to the Al 3p orbital, which induces the magnetic moment of the 3d orbit to be lower than that of Sc_n clusters. It can be seen from table 3 that the 4s orbit of Sc provides a reverse magnetic moment. This causes the magnetic moment decrease. Therefore we think the charge transfer and the strong spd hybridization between Sc 4s, 3d and Al 3s, 3p states might be the major reason for the reduction of the magnetic moment. Moreover, we can see from table 2 that the magnetic moment provided by the Al atom is very small, and even reversed, which also causes the magnetic moment decrease. The exception happens in Sc_8Al and $Sc_{14}Al$ clusters, whose magnetic moments are higher than that of Sc_9 and Sc_{15} clusters, respectively. This might be attributed to the high coordination number and high spin state of the clusters.

4. Conclusions

In summary, we have studied the growth behaviors, stabilities, electronic and magnetic properties of the Sc_nAl, $n = 1$–14 by DFT with the generalized gradient approximation. The resulting geometries show that the aluminum atom remains on the surface of clusters for $n < 9$, but is trapped within the cage of Sc host atoms for $n \geqslant 9$. The stability analysis is carried out

by calculating the average binding energy and the second-order energy differences. The obtained results show that the doping of the Al atom improves the stability of scandium clusters, and Sc_nAl clusters at $n = 3$, 6, 10 and 12 possess relatively higher stability. In addition, the HOMO–LUMO gaps of Sc_nAl clusters are discussed. It is found that the HOMO–LUMO gaps of Sc_nAl clusters containing more than six atoms are very small, and all the HOMO and LUMO states are nondegenerate and delocalized. NPA shows that the 3d electrons play a dominant role for the magnetism of the system. Besides, the doping of the Al atom reduces the magnetic moment of the host clusters except for Sc_9 and Sc_{15} clusters, and the magnetic moment of the Sc_nAl cluster is quenched for $n = 5$, 7, 9 and 11.

Acknowledgments

This work was supported by the Natural Science Foundation of China (no. 90306010), the Program for New Century Excellent Talents in University (no. NCET-04-0653) and the State Key Basic Research '973' Plan of China (no. 2007CB616911).

References

[1] Alonso J A 2000 *Chem. Rev.* **100** 637
[2] Knickelbein M B 2001 *Phys. Rev. Lett.* **86** 5255
[3] Knickelbein M B 2004 *Phys. Rev.* B **70** 014424
[4] Xu X S, Yin S Y, Moro R and de Heer W A 2005 *Phys. Rev. Lett.* **95** 237209
[5] Cox A J, Louderback J G and Bloomfield L A 1993 *Phys. Rev. Lett.* **71** 923
[6] Wei S H, Zeng Z, You J Q, Yan X H and Gong X G 2000 *J. Chem. Phys.* **113** 11127
[7] Kabir M, Mookerjee A and Kanhere D G 2006 *Phys. Rev.* B **73** 224439
[8] Kabir M, Kanhere D G and Mookerjee A 2007 *Phys. Rev.* B **75** 214433
[9] Kondow T and Maufune F 2003 *Progress in Experimental and Theoretical Studies of Clusters* (New York: World Scientific)
[10] Klabunde K J 1994 *Free Atoms, Clusters, and Nanoscale Particles* (New York: Academic)
Klabunde K J 2001 *Nanoscale Materials in Chemistry* (New York: Wiley)
[11] Andrews M P and O'Brien S C 1992 *J. Phys. Chem.* **96** 8233
[12] Jellinek J and Krissinel E B 1999 *Theory of Atomic and Molecular Clusters* (Berlin: Springer) pp 277–308
[13] Jellinek J 2008 *Faraday Discuss.* **138** 11
[14] Wang J L, Wang G H, Chen X S, Lu W and Zhao J J 2002 *Phys. Rev.* B **66** 014419
[15] Bailey M S, Wilson N T, Roberts C and Johnston R L 2003 *Eur. Phys. J.* D **25** 41
[16] Kabir M, Mookerjee A and Kanhere D G 2006 *Phys. Rev.* B **73** 224439
[17] Pramann A, Koyasu K and Nakajima A 2002 *J. Phys. Chem.* A **106** 2483
[18] Xiang J, Wei S H, Yan X H, You J Q and Mao Y L 2004 *J. Chem. Phys.* **120** 4251
[19] Calleja M, Rey C, Alemany M M G and Gallego L J 1999 *Phys. Rev.* B **60** 2020
[20] Baileya M S, Wilson N T, Roberts C and Johnston R L 2003 *Eur. Phys. J.* D **25** 41
[21] Ganguly S, Kabir M, Datta S, Sanyal B and Mookerjee A 2008 *Phys. Rev.* B **78** 014402
[22] Knickelbein M B 2005 *Phys. Rev.* B **71** 184442
[23] Yuan H K, Chen H, Ahmed A S and Zhang J F 2006 *Phys. Rev.* B **74** 144434
[24] Wang J L 2007 *Phys. Rev.* B **75** 155422
[25] Tian F Y, Jing Q and Wang Y X 2008 *Phys. Rev.* A **77** 013202
[26] Verhaegen G, Smoes S and Drowart J 1964 *J. Chem. Phys.* **40** 239
[27] Knight L B Jr, Van Zee R J and Weltner W 1983 *Chem. Phys. Lett.* **94** 296
[28] Moskovits M, DiLella D P and Limm W J 1984 *J. Chem. Phys* **80** 626
[29] Perdew J P 1991 *Electronic Structure of Solids '91* ed P Ziesche and H Eschrig (Berlin: Academic)
Perdew J P, Chevary J A, Vosko S H, Jackson K A, Pederson M R, Singh D J and Fiolhais C 1992 *Phys. Rev.* B **46** 6671
[30] Rosen B 1970 *Spectroscopic Data Relative to Diatomic Molecules* (Oxford: Pergamon)
[31] Delley B 1990 *J. Chem. Phys.* **92** 508
Delley B 2000 *J. Chem. Phys.* **113** 7756 (DMOL is a density functional theory program distributed by Accelrys Inc.)
[32] Hay P J and Wadt W R 1985 *J. Chem. Phys.* **82** 270
Wadt W R and Hay P J 1985 *J. Chem. Phys.* **82** 284
Hay P J and Wadt W R 1985 *J. Chem. Phys.* **82** 299
[33] Frisch M J *et al* 2003 *GAUSSIAN 03* (Pittsburgh, PA: Gaussian)
[34] Zhao G F, Zhang J, Jing Q, Luo Y H and Wang Y X 2007 *J. Chem. Phys.* **127** 234312